# Estimating Respiratory Modulation in Atrial Fibrillation Using a Convolutional Neural Network

Felix Plappert[1], Mikael Wallman[2], Pyotr G Platonov[3], Frida Sandberg[1]

[1] Department of Biomedical Engineering, Lund University, Lund, Sweden
[2] Department of Systems and Data Analysis, Fraunhofer-Chalmers Centre, Gothenburg, Sweden
[3] Department of Cardiology, Clinical Sciences, Lund University, Lund, Sweden

## Abstract

*The quantification of autonomic nervous system (ANS) activity from ECG data may provide useful information for personalizing atrial fibrillation (AF) treatment, but is currently not possible. Since respiration is known to elicit an ANS response, the purpose of this study was to assess whether the respiratory modulation in AV nodal refractory period and conduction delay during AF can be estimated from ECG data. We trained a 1-dimensional convolutional neural network (1D-CNN) on synthetic data generated using a network model of the AV node to estimate the respiratory modulation in AV nodal conduction. The synthetic data replicates clinical ECG-derived data and contained 1-minute segments of RR series, respiration signals and atrial fibrillatory rates (AFR). Further, the synthetic data was generated using a total of 4 million unique parameter sets. We showed using synthetic data that the 1D-CNN can estimate the respiratory modulation from an RR series, respiration signal and AFR with a Pearson sample correlation of* $\rho = 0.855$*. The results of the present study suggest that the proposed method can be used to quantify respiratory-induced variations in ANS activity from ECG data. Further studies are needed to verify the estimates and to investigate the clinical value of the estimates.*

## 1. Introduction

Atrial fibrillation (AF) is the most common supraventricular tachyarrhythmia [1]. During AF, the electrical activation in the atria is uncoordinated and has a faster average rate resulting in an increased and irregular heart rate. Atrial fibrillation is associated with substantial morbidity and mortality, and the personalization of the AF treatment requires a better understanding of the complex mechanisms of AF.

The autonomic nervous system (ANS) is known to contribute to the onset and maintenance of AF [2]. Quantifying the ANS activity during AF could allow for better personalization of treatment. In normal sinus rhythm (NSR), the autonomic tone is usually quantified by heart rate variability (HRV) [3]. However, HRV parameters have a different interpretation in AF because the ventricular rhythm is not initiated in the sinoatrial (SA) node as it is in NSR, but results from the uncoordinated atrial activity and the subsequent modulation of electrical impulses by the AV node. An alternative to HRV may be to investigate the dynamics in the AV nodal conduction because the AV node is densely innervated by the ANS. However, there is currently no methodology utilizing the connection between the AV node and the ANS to quantify the autonomic tone. In this work, we approach this problem by training a 1-dimensional convolutional neural network (1D-CNN) on synthetic data to assess the respiratory modulation in AV nodal conduction properties from ECG data. For the training, we generate synthetic data using an AV node model. The approach of using synthetic data for the training of neural networks for analysis of clinical data has been applied before to overcome the challenge of acquiring large amounts of data, e.g., for the detection of R-waves in ECG signals during different physical activities and atrial fibrillation [4].

The synthetic data was generated using a network model of the AV node. The AV node has two functional pathways with different electrophysiological properties allowing for parallel conduction of impulses [5]. The fast pathway (FP) has a longer refractory period and shorter conduction delay compared to the slow pathway (SP) [5]. Previously, several AV node models have been proposed that focus on different characteristics in the structure and electrophysiology of the AV node, for example [6–9]. Out of all AV node models known to the authors, our previously proposed model [10] is the first to describe ANS-induced changes in AV nodal refractory period and conduction delay. Using that model, we demonstrated that inclusion of ANS-induced changes in the model using a constant scaling of key parameters improves the fit of the predicted RR series to clinical tilt-test measurements. In the present study, we use an

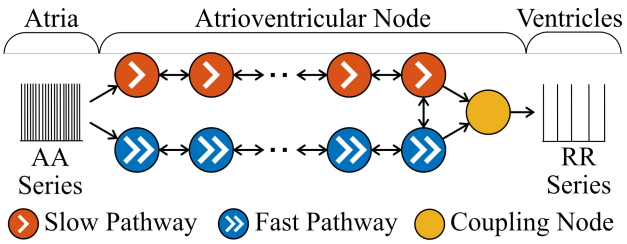


Figure 1. Illustration of the AV node model. Arrows indicate allowed direction of conduction. For simplicity, only a subset of the ten nodes in each pathway is shown.

extended version of that model which incorporates respiratory modulation in AV node conduction properties.

We present the extended AV node model that is used to generate synthetic data. We further present the 1D-CNN that is first trained on the synthetic data and then used to estimate the respiratory modulation in a simulated holdout set, and in clinical data from 28 AF patients performing a deep breathing task. The complete study is described in [11].

## 2. Methods

### 2.1. Model Description

The AV node is modelled as a network of 21 nodes (cf. Fig. 1). The presented AV node model was initially proposed in [9] and extended to account for changes in the autonomic tone, where the model description first allowed static changes to replicate tilt in [10] and then dynamic changes to replicate respiratory modulation in [11]. The dual-pathway physiology with a slow pathway (SP) and fast pathway (FP) is represented with two chains of 10 nodes each. Atrial impulses arrive at the first node of each pathway simultaneously and leave the AV node model over the coupling node (CN). The impulses can travel bidirectionally within the SP and FP, allowing for retrograde conduction. More information about the impulse propagation through the AV node model can be found in [9]. The intervals between atrial impulses entering the AV node during AF used to compute the atrial activation (AA) series are modelled as a point process with independent inter-arrival times distributed according to a Pearson Type IV distribution with a mean $\mu$, standard deviation $\sigma$, skewness $\gamma$ and kurtosis $\kappa$ [12]. The parameters $\mu$ and $\sigma$ were drawn from the bounded uniform distributions $\mathcal{U}[100, 250]$ ms and $\mathcal{U}[15, 30]$ ms, respectively, and $\gamma$ and $\kappa$ were kept fixed at 1 and 6, respectively.

When an impulse arrives at a node, an individual refractory period $R^P(\Delta t_k)$ and conduction delay $D^P(\Delta t_k)$ is computed for this node, defined as

$$R^P(\Delta t_k) = A^P(t)\left(R^P_{min} + \Delta R^P\left(1 - e^{-\Delta t_k/\tau^P_R}\right)\right) \quad (1)$$

$$D^P(\Delta t_k) = A^P(t)\left(D^P_{min} + \Delta D^P e^{-\Delta t_k/\tau^P_D}\right), \quad (2)$$

where $P \in \{SP, FP, CN\}$ indicates the association to a pathway. The $R^P(\Delta t_k)$ and $D^P(\Delta t_k)$ are characterized by six fixed parameters $R^P_{min}$, $\Delta R^P$, $\tau^P_R$, $D^P_{min}$, $\Delta D^P$ and $\tau^P_D$. The model parameters of the SP and FP were drawn from bounded uniform distributions, whereas the parameters of the CN were kept fixed according to Table 1. All nodes in the same pathway use the same fixed parameters and it was ensured that the SP always has a shorter refractory period and longer conduction delay compared to the FP.

Table 1. AV Node model parameters used for simulated data.

| Parameters | | P≡SP (ms) | P≡FP (ms) | P≡CN (ms) |
|---|---|---|---|---|
| $\boldsymbol{\theta}^P_R$ | $R^P_{min}$ | $\mathcal{U}[250, 600]$ | $\mathcal{U}[250, 600]$ | 250 |
| | $\Delta R^P$ | $\mathcal{U}[0, 600]$ | $\mathcal{U}[0, 600]$ | 0 |
| | $\tau^P_R$ | $\mathcal{U}[50, 300]$ | $\mathcal{U}[50, 300]$ | 1 |
| $\boldsymbol{\theta}^P_D$ | $D^P_{min}$ | $\mathcal{U}[0, 30]$ | $\mathcal{U}[0, 30]$ | 0 |
| | $\Delta D^P$ | $\mathcal{U}[0, 75]$ | $\mathcal{U}[0, 75]$ | 0 |
| | $\tau^P_D$ | $\mathcal{U}[50, 300]$ | $\mathcal{U}[50, 300]$ | 1 |

The $R^P(\Delta t_k)$ and $D^P(\Delta t_k)$ are dependent on the previous diastolic interval, described as

$$\Delta t_k = t_k - t_{k-1} - R^P(\Delta t_{k-1}). \quad (3)$$

An impulse is blocked if $\Delta t_k$ is negative, and otherwise conducted to all neighboring nodes.

The respiration-induced changes to the AV nodal conduction properties of the SP and FP is implemented with a scaling factor $A^{SP/FP}(t)$

$$A^{SP}(t) = A^{FP}(t) = 1 + \frac{a_{resp}}{2}\sin(2\pi t f_{resp}), \quad (4)$$

where $a_{resp}$ is the peak-to-peak amplitude of respiratory modulation and $f_{resp}$ is the respiration frequency. The AV nodal conduction properties of the CN are not modulated by respiration and hence $A^{CN} = 1$.

Briefly, to produce a simulated respiration signal, a sine wave with frequency $f_{resp}$ is sampled non-uniformly at the times of ventricular activation produced by the AV node model. Then, Gaussian noise is added to the non-uniform samples after which the signal is resampled to a uniform sampling rate of 4 Hz. A detailed description about how the respiration signals are produced can be found in [11].

## 2.2. Clinical Respiratory Modulation Data

The respiratory modulation of the AV nodal conduction properties in AF was analysed using ECG data recorded during a deep breathing test as part of the SCAPIS study [13]. The clinical dataset contained 12-lead ECG recordings from 28 participants in AF who were resting in supine position while breathing normally for 5 minutes followed by 1 minute of deep breathing with guided cycles of 5 seconds inhalation and 5 seconds exhaltation. The ECG data was divided into 1-minute segments and the RR series $\mathcal{X}_{RR}^{Clin}$ and inverse average atrial fibrillatory rate (AFR) $\mathcal{X}_{AFR}^{Clin}$ were estimated for each segment. Additionally, a respiration signal $\mathcal{X}_{Resp}^{Clin}$ was extracted with a novel method based on the periodic component analysis. The signals were interpolated to a uniform sampling rate of 4 Hz and each signal had the dimension $1 \times 240$. A detailed description of the extraction of RR series, AFR trend and respiration signal can be found in [11].

## 2.3. Simulated Respiratory Modulation Data

Two simulated datasets were created using 2 million unique combinations of AA series and AV node model parameters each, where one dataset was used for training and validation and the other dataset was used for testing of a 1D-CNN (see Sec. 2.4). In the training dataset, $a_{resp}$ was drawn from the bounded uniform distribution $\mathcal{U}[-0.1, 0.5]$ Hz, and in the testing dataset, $a_{resp}$ was drawn from $\mathcal{U}[0, 0.4]$ Hz. The parameter $f_{resp}$ was drawn from $\mathcal{U}[0.1, 0.4]$ Hz for both the training and testing dataset. For each simulation with a unique combination of model parameters, an RR series $\mathcal{X}_{RR}^{Sim}$ was simulated using the AV node model and AA series described in Sec. 2.1, as well as a respiration signal $\mathcal{X}_{Resp}^{Sim}$ and a vector $\mathcal{X}_{AFR}^{Sim}$ containing the model parameter $\mu$. The signals were interpolated to a uniform sampling rate of 4 Hz and each signal had the dimension $1 \times 240$.

## 2.4. Estimation of respiratory modulation

Using one of the simulated datasets, we trained a 1D-CNN in MATLAB to estimate the respiratory modulation $a_{resp}$ ('Deep Learning Toolbox', MATLAB version R2023a, RRID:SCR_001622). The 1D-CNN architecture is illustrated in Figure 2, where the 1D convolution layer consisted of 100 filters with kernel size $k_{\mathcal{C}} = 3$, stride $s_{\mathcal{C}} = 1$ and dilation factor $d_{\mathcal{C}} = 2^{l-1}$, where $l = 1, ..., 5$ denotes the $l$:th convolutional layer in the CNN. The 1D-CNN was trained on the input data $\boldsymbol{\mathcal{X}} = [\mathcal{X}_{RR}^{Sim}; \mathcal{X}_{Resp}^{Sim}; \mathcal{X}_{AFR}^{Sim}]$, where all signals were 1-minute long. Ten realizations were trained with unique training and validation datasets containing 100 000 parameter sets each. A detailed description of the training process of the 1D-CNN can be found in [11]. The $\hat{a}_{resp}$ was computed as the average of the individual estimates from each of the ten 1D-CNN realizations. The 1D-CNN was evaluated using the simulated testing dataset described in Sec. 2.3 with the format $\boldsymbol{\mathcal{X}} = [\mathcal{X}_{RR}^{Sim}; \mathcal{X}_{Resp}^{Sim}; \mathcal{X}_{AFR}^{Sim}]$, and using the clinical dataset described in Sec. 2.2 with the format $\boldsymbol{\mathcal{X}} = [\mathcal{X}_{RR}^{Clin}; \mathcal{X}_{Resp}^{Clin}; \mathcal{X}_{AFR}^{Clin}]$.

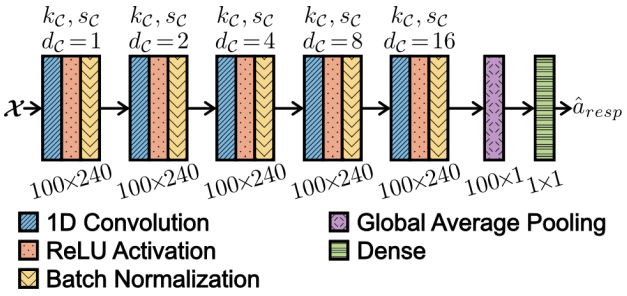


Figure 2. Architecture of the 1D-CNN. The convolution layers had a kernel size $k_{\mathcal{C}} = 3$, stride $s_{\mathcal{C}} = 1$ and dilation factor $d_{\mathcal{C}}$.

# 3. Results

Using the simulated testing dataset, the accuracy of the $a_{resp}$ estimation was assessed for the CNN (cf. Fig 3A). The CNN can estimate $a_{resp}$ with an RMSE of $0.066$, Pearson sample correlation of $\rho = 0.855$, and $R^2$ of $0.674$.

In addition, the CNN was used to estimate $a_{resp}$ from the clinical data (cf. Fig. 3B). In the study population, there was a high interpatient variability in $\hat{a}_{resp}$ and there is a large interpatient variability in the response to deep breathing.

# 4. Discussion and Conclusion

Our results based on the simulated testing dataset show that the 1D-CNN can estimate the respiratory modulation with a strong correlation between estimated $\hat{a}_{resp}$ and true $a_{resp}$ (cf. Fig. 3A). The 1D-CNN cannot be trained on clinical data because the dataset is not sufficiently large. Moreover, we cannot evaluate the performance of $\hat{a}_{resp}$ in clinical data, because $a_{resp}$ is unknown. Due to this, we use simulated data for the training and evaluation of the 1D-CNN and then we use the trained 1D-CNN to estimate $a_{resp}$ in clinical data under the assumption that the simulated data is mimicking the clinical data. Indeed, the AV node model has been shown to replicate clinical data [9, 10, 14], but has not been specifically validated for breathing studies, which is a limitation of the current work. Even though the estimation of respiratory modulation in simulated data shows a strong correlation (cf. Fig. 3A),

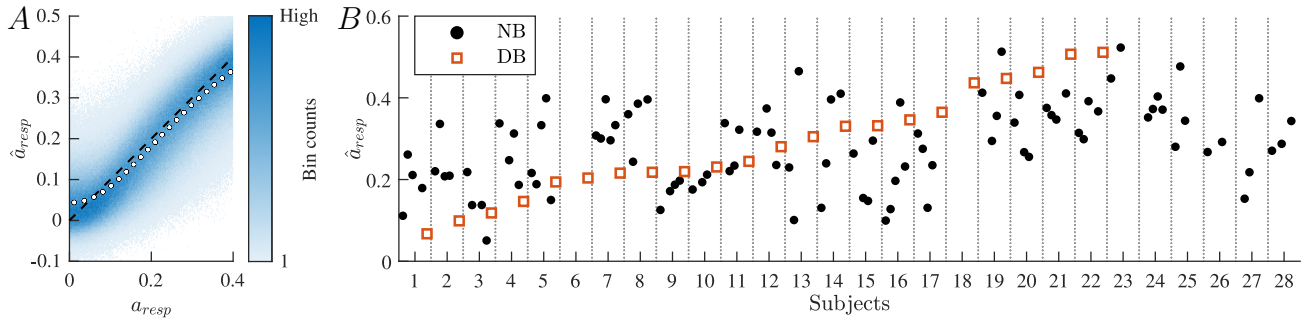


Figure 3. **(A)** Binned scatter plot of estimated $\hat{a}_{resp}$ versus true $a_{resp}$ for the CNN. The black dotted line shows where $\hat{a}_{resp}$ is equal to $a_{resp}$ and the white dotted line shows the sample mean of the $\hat{a}_{resp}$ estimation. **(B)** Black dots correspond to the estimated $\hat{a}_{resp}$ of 1-minute segments during normal breathing (NB) and red squares correspond to $\hat{a}_{resp}$ of 1-minute segments during deep breathing (DB).

we cannot exclude model misspecification as a factor contributing to the large interpatient variability in the estimation results for respiratory modulation in the clinical data (cf. Fig. 3B).

The results of the present study suggest that the proposed method can be used to quantify respiratory-induced variations in ANS activity from ECG data. Further studies are needed to verify the estimates and to investigate the clinical value of the estimates.

## Acknowledgments

The computations were enabled by resources provided by the National Academic Infrastructure for Supercomputing in Sweden (NAISS) and the Swedish National Infrastructure for Computing (SNIC) at Lund University partially funded by the Swedish Research Council through grant agreements no. 2022-06725 and no. 2018-05973. The Swedish Heart and Lung foundation was the main funding body of the SCAPIS cohort. SCAPIS was also supported by grants from the Knut and Alice Wallenberg Foundation, the Swedish Research Council, and Sweden's Innovation agency.

## References

[1] Hindricks G et al. 2020 ESC Guidelines for the diagnosis and management of atrial fibrillation developed in collaboration with the European Association for Cardio-Thoracic Surgery (EACTS). Eur Heart J 2020;42(5):1–126.

[2] Shen MJ and Zipes, Douglas P. Role of the autonomic nervous system in modulating cardiac arrhythmias. Circ Res 2014;114(6):1004–1021.

[3] Sassi R et al. Advances in heart rate variability signal analysis: joint position statement by the e-Cardiology ESC Working Group and the European Heart Rhythm Association co-endorsed by the Asia Pacific Heart Rhythm Society. EP Europace 2015;17(9):1341–1353.

[4] Kaisti M et al. Domain randomization using synthetic electrocardiograms for training neural networks. Artif Intell Med 2023;143:102583.

[5] George SA et al. At the atrioventricular crossroads: dual pathway electrophysiology in the atrioventricular node and its underlying heterogeneities. Arrhythmia Electrophysiol Rev 2017;6(4):179–185.

[6] Cohen, RJ et al. A quantitative model for the ventricular response during atrial fibrillation. IEEE Trans Biomed Eng 1983;30(12):769–781.

[7] Henriksson M et al. A statistical atrioventricular node model accounting for pathway switching during atrial fibrillation. IEEE Trans Biomed Eng 2016;63(9):1842–1849.

[8] Inada S et al. Simulation of ventricular rate control during atrial fibrillation using ionic channel blockers. J Arrhythm 2017;33(4):302–309.

[9] Wallman, M and Sandberg, F. Characterisation of human AV-nodal properties using a network model. Med Biol Eng Comput 2018;56(2):247–259.

[10] Plappert F et al. An atrioventricular node model incorporating autonomic tone. Front Physiol 2022;13:976468.

[11] Plappert F et al. ECG-based estimation of respiratory modulation of AV nodal conduction during atrial fibrillation. arXiv 2023;doi:10.48550/arXiv.2309.05458.

[12] Climent AM et al. Generation of realistic atrial to atrial interval series during atrial fibrillation. Med Biol Eng Comput 2011;49(11):1261–1268.

[13] Bergström, G et al. The Swedish CArdioPulmonary BioImage Study: objectives and design. J Intern Med 2015; 278(6):645–659.

[14] Karlsson M et al. ECG based assessment of circadian variation in AV-nodal conduction during AF – Influence of rate control drugs. Front Physiol 2022;976526.

Address for correspondence:

Felix Plappert
Lund University, Department of Biomedical Engineering
Box 118, 221 00 Lund, Sweden
felix.plappert@bme.lth.se